

NASA Technical Memorandum 106549

# Performance and Durability of High Emittance Heat Receiver Surfaces for Solar Dynamic Power Systems

Kim K. de Groh  
*Lewis Research Center*  
*Cleveland, Ohio*

David M. Roig and Christopher A. Burke  
*Cleveland State University*  
*Cleveland, Ohio*

and

Dilipkumar R. Shah  
*AlliedSignal Aerospace Company*  
*Torrance, California*

Prepared for the  
1994 ASME International Solar Energy Conference  
sponsored by the American Society of Mechanical Engineers  
San Francisco, California, March 27-30, 1994



National Aeronautics and  
Space Administration

Revised Copy

Trade names or manufacturers' names are used in this report for identification only. This usage does not constitute an official endorsement, either expressed or implied, by the National Aeronautics and Space Administration.

# Performance and Durability of High Emittance Heat Receiver Surfaces for Solar Dynamic Power Systems

Kim K. de Groh

National Aeronautics and Space Administration  
Lewis Research Center  
Cleveland, Ohio 44135

David M. Roig & Christopher A. Burke  
Cleveland State University  
Cleveland, Ohio 44115

Dilipkumar R. Shah  
AlliedSignal Aerospace Company  
Torrance, California 90509

## SUMMARY

Haynes 188, a cobalt-based superalloy, will be used to make thermal energy storage (TES) containment canisters for a 2 kW solar dynamic ground test demonstrator (SDGTD). Haynes 188 containment canisters with a high thermal emittance ( $\epsilon$ ) are desired for radiating heat away from local hot spots, improving the heating distribution, which will in turn improve canister service life. In addition to needing a high emittance, the surface needs to be durable in an elevated temperature, high vacuum ( $\approx 830^\circ\text{C}$ ,  $<10^{-7}$  torr) environment for an extended time period.

Thirty-five Haynes 188 samples were exposed to 14 different types of surface modification techniques for emittance and vacuum heat treatment (VHT) durability enhancement. Optical properties were obtained for the modified surfaces. Emittance enhanced samples were exposed to VHT for up to 2692 hr at  $827^\circ\text{C}$  and  $\leq 10^{-6}$  torr with integral thermal cycling. Optical properties were taken intermittently during exposure, and after final VHT exposure.

The various surface modification treatments increased the emittance of pristine Haynes 188 from 0.11 to between 0.28 and 0.86. Seven different surface modification techniques were found to provide surfaces which meet the SDGTD receiver VHT durability requirement ( $\epsilon \geq 0.70$  after 1000 hr). Of the 7 surface treatments, 2 were found to display excellent VHT durability: alumina-titania (AlTi) coatings ( $\epsilon = 0.85$  after 2695 VHT hrs) and zirconia-titania-yttria coatings ( $\epsilon = 0.86$  after 2024.3 VHT hr). The AlTi coating was chosen for the enhancement surface modification technique for the SDGTD receiver. Details of the alumina-titania coating and other Haynes 188

emittance surface modification techniques are discussed. Technology from this program will lead to successful demonstration of solar dynamic power for space applications, and has potential for application in other systems requiring high emittance surfaces.

## INTRODUCTION

Solar dynamic power systems have been investigated for electrical power generation on Space Station Freedom (SSF) and other space systems. In a solar dynamic power system, a solar concentrator reflects focused solar energy into a receiver to operate a heat engine. Solar dynamic systems investigated by NASA for use on SSF would use a closed-Brayton cycle heat engine, generating 25 kW of power (ref. 1). A 2 kW prototype solar dynamic ground test demonstrator is currently being built to demonstrate solar dynamic technology (ref. 2). The SDGTD, managed by NASA Lewis Research Center (LeRC), will demonstrate production of solar dynamic power for 1000 hours in LeRC's large thermal/vacuum space environmental facility (see fig. 1) (ref. 2). Completion of fabrication of the 2 kW system and its initial testing is scheduled for Spring of 1995 (ref. 2).

The heat receiver for the SDGTD system is based on the design investigated for the SSF 25 kW system (refs. 3 and 4). Inside the receiver (see fig. 2), solar energy is transferred to a Xe-He gaseous working fluid in a closed-Brayton heat engine through thermal energy storage containment canisters (ref. 4). The canisters contain TES material, also known as phase change material (PCM), which stores the heat of fusion of a mixture of salts



(LiF-CaF<sub>2</sub> eutectic salt) to provide heat for power generation during the substantial eclipse portion of the orbit.

The receiver TES containment canisters and working fluid tubes are being made of Haynes 188, a cobalt-based superalloy. Haynes 188 containment canisters with a high thermal emittance surface are desired for radiating heat away from local hot spots. This will greatly improve the heating distribution inside the receiver and improve canister service life. Because the heat receiver will operate at elevated temperatures ( $\approx 827^\circ\text{C}$ ) in a vacuum environment ( $\leq 10^{-6}$  torr) in both space and in the simulated space chamber, the high emittance surface needs to be durable in these hostile environments and resist optical property degradation. Surface chemistry and morphological changes which may occur due to sublimation, diffusion and thermal relaxation at elevated temperature under vacuum could adversely affect optical properties. Research programs were initiated first in 1989 under the SSF SD program with the Electro-Physics Branch at NASA LeRC, and recently under the SDGTD program jointly with the Electro-Physics Branch at NASA LeRC and AlliedSignal Aerospace Company to investigate development of durable high emittance Haynes 188 surfaces for heat receiver applications.

The SSF emittance program investigated various surface modification techniques to improve the Haynes 188 surface emittance. Under this program, four samples were exposed to extended elevated temperature ( $827^\circ\text{C}$ ) vacuum heat treatment (VHT) (ref. 5). Samples were also evaluated for elevated temperature atomic oxygen durability (ref. 5). It was found that SiC grit blasting the Haynes surface followed by air oxidation produced a high emittance surface. The oxidized surfaces were found to provide initial protection against sublimation-related surface changes, but the oxide was found to be unstable over extended elevated temperature vacuum exposures (5215.5 hr) and the protection was not permanent (ref. 5). The SDGTD emittance program was initiated to continue investigations of Haynes 188 surface modification, with a stronger emphasis on developing a high emittance surface which would be environmentally durable, with little or no change in emittance after 1000 hr of VHT exposure.

Under the SDGTD emittance program, 35 Haynes 188 samples were exposed to 14 different types of surface modification techniques for emittance and vacuum heat treat durability enhancement. The emittance enhancement techniques included grit blasting followed by air oxidation, arc texturing, mechanically indenting followed by air oxidation, laser treatment, detonation gun and plasma spray coatings. Additionally, SiO<sub>2</sub> and Al<sub>2</sub>O<sub>3</sub> coatings were applied for durability enhancement. Emittance, absorptance and mass measurements were obtained for the modified surfaces. Emittance-enhanced test

samples were exposed to vacuum heat treatment (VHT) for up to 2692 hr at  $827^\circ\text{C}$  and  $\leq 10^{-6}$  torr. Samples were also thermal cycled during VHT between  $827^\circ\text{C}$  and room temperature at  $\approx 100$  hr intervals. Optical property measurements were taken intermittently during exposure, and after final VHT exposure. Details of the emittance performance of samples which underwent various surface modification techniques are explored along with their VHT durability, and the recommended surface modification for use on the SDGTD receiver are discussed in this paper.

## EXPERIMENTAL PROCEDURES

### Material

Surface modifications and optical property characterizations were conducted on 2.53 cm diameter, 0.16 cm thick Haynes 188 sample coupons. Haynes 188, contains  $\approx 38.0$  percent (by weight) Co, 23.03 percent Ni, 21.69 percent Cr, 14.02 percent W, 1.95 percent Fe,  $< 1$  percent Mn, Si, P, C, La, and trace amounts of B and S.

### Surface Modification Techniques for Emittance Enhancement

#### Surface Texturing

Grit Blasting and Air Oxidation: Grit blasting with  $60\ \mu\text{m}$  SiC grit followed by air oxidation was re-evaluated based on the good emittance values obtained under the SSF emittance program (ref. 5). The SSF emittance program indicated that the oxide film formed during air oxidation became embrittled and nonadherent after long term VHT (5215.5 hrs at  $827^\circ\text{C}$ ) (ref. 5). Therefore, it was believed that a thinner oxide film would maintain better adherence, and hence better  $\epsilon$ , with anticipated thermal cycling. Several temperature and time variations were examined in an attempt to evaluate the effect of variation in oxide thickness on emissivity under long term VHT exposure. The various temperature/time combinations evaluated were: (a)  $982^\circ\text{C}$  for 2 hr, 4 hr and 16 hr, and (b)  $871^\circ\text{C}$  for 3 hr, 6 hr and 24 hr.

Physical Texturing: Other types of physical deformation techniques were explored to increase the surface roughness and therefore the thermal emittance of the Haynes 188 surface. One sample was mechanically indented by a mechanical vibration pen. This sample was then subjected to air oxidation ( $871^\circ\text{C}/24$  hr) for further emittance enhancement. A second sample was mechanically indented with application of graphite in an attempt to simulate carbon inclusion into the surface like arc texturing described below. A third sample was prepared



using computer controlled laser etching over the surface of the Haynes coupon, until a uniform texture appearance was obtained.

**Arc Texturing:** A combination of physical roughening and chemical altering was explored by arc texturing the Haynes surface. Carbon-rod arc texturing has been demonstrated to produce a high emittance surface for space radiator applications (ref. 6). Arc texturing was accomplished by producing an electric arc discharge between an electrode (typically C) and the Haynes substrate material. A uniform texture was produced by slowly moving the arc over the sample surface in either air or an inert atmosphere until a uniform dark appearance was achieved. Metal from the Haynes 188 surface and the arc electrode material (C or SiC) vaporizes during arcing and condenses onto the Haynes surface to produce a microscopically rough surface (ref. 6). Both C and SiC electrodes were used, with the C arc texturing performed in an argon atmosphere, and SiC arc texturing performed in air. Although arc texturing using a carbon electrode is most common, SiC was investigated in attempt to provide the chemistry which would allow development of an adherent SiC protective layer that could convert to  $\text{SiO}_2$  during VHT.

#### Coatings for Emittance Enhancement

**ZTY and ZYH Coatings:** Two coatings used for thermal barrier applications were evaluated for emittance enhancement with potential integral VHT durability. These coatings with typical compositions are: (a) zirconia (72 percent)/titania (18 percent)/yttria (10 percent) (ZTY) and (b) zirconia (90 percent)/yttria (8 percent)/hafnia (2 percent) (ZYH). The coatings were applied using plasma spray techniques. Both coatings were originally deposited with 0.254 mm thicknesses. However, thermal barrier concerns for this application resulted in preparation and evaluation of ZTY coated samples with thinner coatings. The effect of thickness on both the optical performance and VHT durability was evaluated. These additional ZTY coatings were 0.025, 0.056, 0.071, and 0.104 mm thick.

**Alumina-Titania Coatings:** Alumina-titania coatings, 60 wt %  $\text{Al}_2\text{O}_3$  - 40 wt %  $\text{TiO}_2$ , were also evaluated for potential combined emittance enhancement with integral VHT durability. The AlTi coatings were applied using a Praxair detonation gun process. Two thicknesses of AlTi coatings were evaluated (0.025 and 0.051 mm). Samples were grit blasted prior to coating.

#### Protective Coatings for Durability Enhancement ( $\text{SiO}_2$ and $\text{Al}_2\text{O}_3$ )

The SSF emittance study provided evidence of sublimation of Haynes 188 high vapor pressure materials (Cr,

Co, & Ni) (ref. 5). Therefore, it was decided to evaluate the application of protective coatings on top of grit blast and air oxidized samples and also on the C arc textured samples. The protective coatings were expected to protect the underlying high emittance surface by forming a diffusion barrier and/or acting as a sacrificial sublimation layer and reduce the degradation of optical properties of the high emittance surface. Two metal oxide thin film protective layers,  $\text{SiO}_2$  and  $\text{Al}_2\text{O}_3$ , were evaluated. Because the protective coatings were applied onto microscopically rough surfaces, both physical vapor deposition (PVD) which produces line-of-site deposition, and chemical vapor deposition (CVD) which produces conformal deposition, were evaluated for protective ability.

The PVD technique used was electron beam evaporation. To help promote uniform coverage during electron beam evaporation, the samples were coated at  $45^\circ$  angles, then rotated  $90^\circ$  and coated again. The precursor material for CVD deposition of  $\text{SiO}_2$  was tetraethoxysilane with an argon carrier gas. The substrate temperature was maintained at  $300^\circ\text{C}$ , and the pressure was kept at 0.8 to 0.9 torr. The precursor for CVD deposition of  $\text{Al}_2\text{O}_3$  was aluminum triisopropoxide. The substrate temperature was kept at  $325^\circ\text{C}$ , and the pressure was kept at 0.8 torr. Both CVD and PVD protective coatings were between 1000 and 1300 Å thick.

#### Characterization

**Optical Properties.** Thermal emittance at  $827^\circ\text{C}$  ( $\epsilon_{827^\circ\text{C}}$ ) was originally obtained using data from both a Hohlraum Reflectometer and a Perkin-Elmer  $\lambda$ -9 Spectrophotometer. The Hohlraum Reflectometer was used to obtain spectral emittance over the wavelength range from 1700 to 14,700 nm. The  $\lambda$ -9 was used to obtain spectral emittance over the wavelength range 400 to 2500 nm. The spectral data from both instruments were weighted in the overlap area, and the integrated thermal emittance at  $827^\circ\text{C}$  was obtained by convoluting this spectrum into the blackbody distribution function at  $827^\circ\text{C}$  (ref. 7). Thermal emittance uncertainty is  $\pm 10$  percent. Although this was the desired method for obtaining thermal emittance, unavailability of the Hohlraum Reflectometer during the remainder of testing resulted in obtaining data on the spectral emittance at  $827^\circ\text{C}$ .

The spectral emittance at  $827^\circ\text{C}$  ( $\epsilon_{827^\circ\text{C}*}$ ) was obtained using the  $\lambda$ -9 Spectrophotometer. Hemispherical reflectance was measured at 2634 nm, the wavelength of the peak emissive power of the  $827^\circ\text{C}$  blackbody curve. The spectral absorptance ( $\alpha_\lambda$ ) at 2634 nm was obtained by subtracting the spectral reflectance from 1. The spectral emittance for  $827^\circ\text{C}$  was then obtained based on Kirchhoff's Law ( $\epsilon_\lambda = \alpha_\lambda$ ) (ref. 8). Spectral reflectance



uncertainty is  $\pm 2$  percent. Comparisons of spectral emittance at 827 °C and integrated thermal emittance at 827 °C for several samples showed good correlation (typically within  $\pm 3$  percent). Because the thermal emittance durability was a critical issue, it was decided this technique was appropriate for determining emittance changes with VHT exposure.

Solar absorptance was obtained on a Perkin-Elmer  $\lambda$ -9 Spectrophotometer operated with a 60 mm integrating sphere. Total spectral reflectance was obtained over the wavelength range 250 to 2500 nm. Integrated solar hemispherical reflectance was obtained by convoluting the spectrum into the air mass zero (AM0) solar spectrum over the same range. Solar absorptance was then calculated by subtracting the solar hemispherical reflectance from 1. A few of the acquired spectra were convoluted into the SDGTD solar simulator spectrum (for a xenon arc-lamp) to compare AM0 solar absorptance with solar simulator absorptance.

**Oxide Thickness.** The oxide thickness of two grit blast and air oxidized samples (982 °C for 4 and 16 hr) was determined. These samples were cross-sectioned, mounted, and metallographically prepared for optical microscopy examination. The oxide thickness resulting from the two air oxidation treatments was then determined by measuring oxide thickness from micrograph images obtained at 1000 X.

### Vacuum Heat Treatment

Surface treated samples were heated to 820 °C in a vacuum environment of  $\leq 10^{-6}$  torr between 1159.3 and 2692 hr. Test samples did not receive identical exposure durations because various samples were fabricated and introduced into the vacuum furnace over a period of time. The SSF emittance program provided evidence of embrittlement of the heat treated high emittance surface (ref. 5). It was anticipated that thermal cycling may accelerate optical property degradation through spalling of the embrittled surfaces. Therefore, thermal vacuum exposure was programmed to include 100 hr thermal cycles (820 °C to room temperature) without breaking vacuum. Thermal cycling at 100 hr intervals simulates the anticipated cycling which could occur during SDGTD operation. Thermal cycling interruptions with corresponding vacuum breaks were experienced due to facility shutdowns, planned interruptions for sample characterization, or introduction of more samples into the thermal vacuum facility. Optical property and mass measurements were taken periodically during VHT exposure.

## RESULTS AND DISCUSSION

### Optical Properties ( $\epsilon$ and $\alpha_s$ ) prior to VHT

**Effect of Surface Modification on  $\epsilon$  and  $\alpha_s$ .** The thermal emittance at 827 °C (827 °C), spectral emittance at 827 °C ( $\epsilon_{827^\circ\text{C}^*}$ ) and solar absorptance ( $\alpha_s$ ) for pristine Haynes 188 were 0.14, 0.08 and 0.370, respectively. The results of the various surface modifications on the as treated optical properties of Haynes 188 are summarized in table I. A bar graph, shown in figure 3, graphically shows the range and tailorability of the Haynes 188 emittance through surface modification. Table I does not include samples which were coated with  $\text{SiO}_2$  or  $\text{Al}_2\text{O}_3$  protective coatings. In this graph, and all following graphs,  $\epsilon$  is given as an average of  $\epsilon_{827^\circ\text{C}}$  and  $\epsilon_{827^\circ\text{C}^*}$  for pristine samples when both values are available, whereas  $\epsilon_{827^\circ\text{C}^*}$  is given for VHT values. It should be noted that for each surface treatment, the pristine values ( $\epsilon_{827^\circ\text{C}}$ ,  $\epsilon_{827^\circ\text{C}^*}$ , and  $\alpha_s$ ) were not necessarily obtained from the same sample.

Comparisons of AM0 solar absorptance (data integrated with respect to the solar spectrum at AM0), and solar simulator absorptance (data integrated with respect to the solar simulator spectrum), were made for the AlTi coated samples. The variation between the values were within experimental error; therefore, solar absorptance values originally obtained are listed instead of solar simulator values.

The desired thermal emittance for the SDGTD receiver canisters is 0.80. Four different surface modification techniques were found to increase the emittance of Haynes 188 from 0.14 to 0.80 or above. These surface modification treatments are: the application of an alumina-titania coating, carbon arc texturing, SiC arc texturing, and SiC grit blasting followed by air oxidation at 871 °C, as shown in table I and figure 3. The  $\epsilon$  values for samples treated with laser etching and prepared with ZYH coatings are low (0.40 and 0.28, respectively) and are not discussed further.

**Effect of Air Oxidation Temperature and Time on  $\epsilon$  and  $\alpha_s$ .** Air oxidizing at 871 °C gave better optical performance ( $\epsilon$  and  $\alpha_s$ ) than air oxidizing at 982 °C. Grit blasting followed by air oxidation at 871 °C for 3, 6, or 24 hr resulted in an  $\epsilon$  of  $0.79 \pm 0.02$  and  $\alpha_s$  of  $0.905 \pm 0.007$ . Grit blasting followed by air oxidation at 982 °C for 2, 4, or 16 hr resulted in an  $\epsilon$  of  $0.72 \pm 0.01$  and  $\alpha_s$  of  $0.892 \pm 0.003$ . There also appears to be a trend for slightly higher  $\epsilon$ , but not higher  $\alpha_s$ , for the samples with shorter oxidation times at either 871 or 982 °C. Table II lists the individual air oxidized samples and their resulting optical properties.



The oxide thicknesses measured for the 2 samples oxidized at 982 °C for 4 and 16 hr were  $2.8 \pm 0.4 \mu\text{m}$  and  $3.9 \pm 0.1 \mu\text{m}$ , respectively. Optical microscopy revealed two oxide layers, an inner layer believed to be  $\text{Cr}_2\text{O}_3$ , and an outer layer believed to be a spinodal composition. The inner layer was almost the same thickness for the two samples ( $1.3 \pm 0.1 \mu\text{m}$  for 4 hr, and  $1.2 \pm 0.1 \mu\text{m}$  for 16 hr), while the outer layer varied in thickness ( $1.5 \pm 0.4 \mu\text{m}$  for 4 hr and  $2.7 \pm 0.1 \mu\text{m}$  for 16 hr).

**Mechanical Texturing versus Grit Blasting Prior to Oxidation.** Silicon carbide grit blasting followed by air oxidation at 871 °C for 24 hr resulted in significantly better optical performance than mechanically indenting, followed by air oxidation for the same time and temperature. As can be seen in table II, the  $\epsilon$  and  $\alpha_s$  for grit blasting prior to air oxidation was 0.77 and 0.912, respectively, and 0.68 and 0.890 for mechanically indenting prior to air oxidation.

**Effect of Coating Thickness (ZTY and AlTi) on  $\epsilon$  and  $\alpha_s$ .** Table III lists 2 AlTi coating thicknesses, and 5 ZTY coating thicknesses, and the corresponding optical properties for the as deposited coatings. For both AlTi and ZTY, the coating thickness did not have a notable effect on the optical properties. The thinner (0.025 mm) ZTY coatings had slightly higher  $\epsilon$  and  $\alpha_s$  values of 0.75 and 0.879, respectively, than the thicker coatings (0.254 mm) with  $\epsilon$  and  $\alpha_s$  of 0.72 and 0.852, respectively. Composition variations from batch to batch may contribute to these differences. Based on as-deposited performance, thinner coatings of AlTi and ZTY would be more desirable due to lower thermal barrier effects. However, calculations from a one-dimensional infinite slab thermal analysis that evaluated the effect of coating thickness on a Haynes substrate has shown that either of these coatings could be applied at 0.254 mm thickness with a negligible effect on heat transfer to the TES salt and working fluid.

**C versus SiC Arc texturing versus Mechanical Indenting with Graphite Application.** Both C and SiC electrode arc texturing resulted in very high  $\epsilon$  and  $\alpha_s$  values, see table IV. As mentioned previously, C arc texturing resulted in an average  $\epsilon$  of 0.82 and an  $\alpha_s$  of 0.906. Silicone carbide arc texturing resulted in an  $\epsilon$  of 0.80 and an  $\alpha_s$  of 0.914. These values could vary from one sample to another because they are arc textured in a sweeping motion until they appear to darken no further. Because this was done by hand, judgement of complete darkening introduces human error. This variation is apparent in the carbon arc textured sample values. The  $\epsilon_{827^\circ\text{C}}$  and  $\epsilon_{827^\circ\text{C}*}$  values obtained from two different samples are quite different (0.77 and 0.86, respectively).

Mechanically indenting with application of graphite, in an attempt to simulate C incorporation into the surface such as arc texturing accomplishes, did not result in very good optical properties. The  $\epsilon$  and  $\alpha_s$  are only 0.42 and 0.516, respectively. This technique was considered unsuccessful compared to arc texturing.

**Effect of  $\text{SiO}_2$  or  $\text{Al}_2\text{O}_3$  Protective Coatings on  $\epsilon$  and  $\alpha_s$ .** For the SiC grit blasted and air oxidized samples, the subsequent application of an  $\text{SiO}_2$  or  $\text{Al}_2\text{O}_3$  protective coating resulted in a variation of effects on the optical properties. For shorter air oxidation times at both 871 °C and 982 °C (2 to 6 hr) the application of a CVD  $\text{SiO}_2$  coating resulted in a decrease in  $\epsilon$ , see table II. The amount of absolute decrease varied from 0.03 and 0.04 for 871 °C (3 and 6 hr, respectively), to 0.16 and 0.17 for 982 °C (2 and 4 hr, respectively). For the longer air oxidation time at 871 °C (24 hr), the  $\epsilon$  increased slightly from 0.77 to 0.80 and 0.79 for PVD and CVD  $\text{SiO}_2$  coatings, respectively, and remained the same with a CVD  $\text{Al}_2\text{O}_3$  coating. While the  $\epsilon$  increased from 0.71 to 0.73 for 982 °C at 16 hr with a PVD  $\text{SiO}_2$  coating and decreased to 0.58 with a CVD  $\text{SiO}_2$  coating.

In summary, the application of a PVD  $\text{SiO}_2$  coating increased the  $\epsilon$  slightly, while the application of a CVD  $\text{SiO}_2$  coating generally decreased the  $\epsilon$  from a slight amount to a large extent. There are two possible explanations for these effects. The first possibility is the variation of defects and impurities in the deposited oxide coating with the individual techniques. Small amounts of C and H from the precursor material are known to be incorporated into CVD  $\text{SiO}_2$  coatings. Defects and impurities cause optical property changes such as color center formations (ref. 9). The second possible explanation for the large variations in emittance may be due to variations in the oxide thickness. For example, there is significant fluctuation in the spectral emittance of silica on a silicon substrate as a function of oxide thickness (ref. 10). Reference 10 shows the spectral emittance at  $\lambda = 694.3 \text{ nm}$  ( $T = 1300^\circ\text{C}$ ) fluctuating from  $\approx 0.58$  to 0.85 for every  $\approx 112 \text{ nm}$  additional thickness of silica. Each of these effects may be sufficient alone to cause the observed emittance variations, but it is more likely to be a synergistic effect of the two.

### Optical Properties ( $\epsilon$ and $\alpha_s$ ) after VHT

**Effect of Air Oxidation Temperature and Time on VHT Durability.** There was a significant effect of oxidation temperature and time, on the VHT durability of grit blast and air oxidized Haynes 188 samples. As can be seen in figure 4, the sample likely to have the thickest



oxide (982 °C for 16 hr) was found to be very durable, with no degradation in  $\epsilon$ , after VHT exposure for 2044.2 hr. The sample with the presumably thinnest oxide (871 °C for 3 hr) was found to degrade very rapidly with the worst VHT durability performance. These results indicate that in addition to providing a high emittance, air oxidizing forms an inherent protective coating with the protective ability depending on the oxide thickness. The formation of a protective coating is in agreement with the previous findings from the SSF emittance program (ref. 5) and alloy evaporation studies by Bourgette (ref. 11). The 982 °C/16 hr air oxidized sample exposed in the current emittance program received 20 thermal cycles, and this sample along with all other air oxidized samples, indicated no signs of embrittlement or spalling after 2044.2 hr VHT exposure. These findings do not support the previously mentioned belief that a thinner oxide would maintain better adherence and hence better  $\epsilon$  with thermal cycling. The oxide embrittlement displayed in the SSF emittance program (ref. 5) may be attributed to the additional exposure time (total of 5215.5 hr), or may have been affected by the Al, Ca and Mg contamination which occurred during VHT exposure.

**Effect of SiO<sub>2</sub> and Al<sub>2</sub>O<sub>3</sub> Protective Coatings on VHT Durability.** For samples which were grit blasted and then air oxidized at 871 °C for 24 hr, the subsequent application of a PVD SiO<sub>2</sub> coating provided a slight improvement in the VHT durability compared to the sample with no additional protective coating (see fig. 5). But, for an unexplained reason, the application of either a CVD SiO<sub>2</sub> coating or a CVD Al<sub>2</sub>O<sub>3</sub> coating decreased the VHT durability. As can be seen in figure 5, the CVD Al<sub>2</sub>O<sub>3</sub> coating performed slightly worse compared to the CVD SiO<sub>2</sub> coating. Because the vapor pressure of Al<sub>2</sub>O<sub>3</sub> is lower than SiO<sub>2</sub>, the opposite effect was expected. Although a CVD SiO<sub>2</sub> coating was found to degrade the VHT durability of the sample air oxidized at 871 °C for 24 hr, neither a PVD nor a CVD SiO<sub>2</sub> coating significantly harmed or helped the VHT durability of the sample air oxidized at 982 °C for 16 hr (see fig. 6). In this case, there was a slight advantage of the CVD coating over the PVD coating.

The application of additional protective coatings (SiO<sub>2</sub>, Al<sub>2</sub>O<sub>3</sub>) to samples with thick air oxidized surfaces (982 °C/16 hr and 871 °C/24 hr) gave inconsistent results. Both small benefits and harmful effects were observed. For samples air oxidized with thin oxide surfaces, three out of four samples (871 °C/3 hr, 982 °C/2 hr and 982 °C/4 hr) showed significant increases in the VHT durability with the addition of a CVD SiO<sub>2</sub> protective layer (see fig. 7). In general, the application of SiO<sub>2</sub> protective coatings benefits air oxidized samples with thin oxide surfaces,

but air oxidized surfaces with thick oxides form inherent protective coatings, and additional SiO<sub>2</sub> coatings do not provide any additional benefit.

Another trend noticed was that samples with oxidized surfaces (either the air oxidized or deposited protective oxide) with low  $\epsilon$ , tend to increase in  $\epsilon$  with initial VHT exposure. While those with initially high  $\epsilon$  ( $\approx 0.80$ ) only decrease with VHT exposure. In addition, the samples which start with a lower  $\epsilon$  and increase with VHT exposure then tend to be more durable than those with an initially high  $\epsilon$ . This trend can be observed in figures 4 and 7.

**Comparison of C and SiC Arc texturing VHT Durability.** The unexposed carbon arc textured surface appeared uniformly black and had a high  $\epsilon$  (average of 0.82). Unfortunately this sample was found to degrade rapidly with VHT exposure, as can be seen in figure 8. The surface after VHT exposure was very light colored, and it appeared that the incorporated carbon was evaporated from the surface, resulting in the  $\epsilon$  decrease. Because of the loss of the C, SiC arc texturing was evaluated with the hope that SiC would be incorporated into the Haynes surface and a SiO<sub>2</sub> protective layer would develop with background oxygen during VHT exposure. The SiC arc textured surface was found to be more VHT durable than the C arc textured surface, but the SiC arc textured surface also degraded rapidly with VHT exposure (see fig. 8). This surface also changed from a black appearance to a light appearance with VHT exposure.

The application of CVD and PVD SiO<sub>2</sub> protective coatings onto the C arc textured surface resulted in improved VHT durability as can be seen in figure 8. In this case, the CVD coating process was found to provide much greater protection than the PVD process. These results are consistent with anticipated results for PVD and CVD protective coatings. Even the best arc textured performer, CVD SiO<sub>2</sub> coated C arc textured, was found to drop significantly in  $\epsilon$  with VHT exposure, making arc texturing undesirable even though the initial  $\epsilon$  was very high.

**Effect of Coating Thickness (ZTY and AlTi) on VHT Durability.** The initial  $\epsilon$  values of the ZTY coated Haynes samples were between 0.71 and 0.75. These values were found to increase rather significantly with VHT exposure (see fig. 9). The 0.254 mm thick ZTY coatings increased to 0.89 after 316.5 hr, and the 0.025 to 0.104 mm thick ZTY coatings increased to 0.85 after 555.5 hr of VHT exposure. These effects are attributed to stoichiometric changes which occur under VHT exposure (ref. 9). These samples were found to be very durable to VHT exposure. The 0.025 to 0.104 mm thick ZTY coated samples reacted very similarly to each other with no coating thickness effect, as can be seen in figure 9, and



had an average resulting  $\epsilon$  of 0.83 after 1159.3 hr and 13 thermal cycles. This value is higher than the average initial value of 0.73. The 2 samples coated with 0.254 mm thick ZTY performed even better than the thinner coats, with a final  $\epsilon$  of 0.86 after 2024.3 hr of VHT exposure with 25 thermal cycles. There was no physical degradation (embrittlement, coating spalling, etc.) noticed with these samples.

The AlTi coated samples, 0.025 and 0.051 mm thick, were found to be very VHT durable. Both of these samples started with a very high initial  $\epsilon$  of 0.86 and then further increased to 0.89 after 984.2 hr of VHT exposure (see fig. 10). Again, this is probably attributed to stoichiometric changes with VHT exposure. These samples, reacting almost identically, were then found to drop in  $\epsilon$  to only 0.85, essentially the initial  $\epsilon$ , after 2692 hr of VHT exposure with 32 thermal cycles. There was no physical degradation noticed with the AlTi coatings.

**Comparison of Surface Modification VHT Durabilities.** The three graphs in figure 11 display the  $\epsilon$  VHT durability for all 35 samples tested. The requirement for the SDGTD receiver was to maintain an  $\epsilon$  of at least 0.70 for 1000 hr. The samples are graphed in the order in which they were introduced into the vacuum furnace. Lines are drawn on the graphs at 1000 hr and  $\epsilon = 0.70$  to help visualize which samples meet the specified requirements. A total of 12 samples were found to maintain an  $\epsilon$  of at least 0.7 after 1000 hr of VHT exposure; 2 from figure 11(a) (982 °C/16 hr and 982 °C/16 hr PVD SiO<sub>2</sub> coated), 4 from figure 11(b) (982 °C/4 hr CVD SiO<sub>2</sub> coated, 982 °C/16 hr CVD SiO<sub>2</sub> coated, AlTi 0.025 and AlTi 0.051 mm), and 6 from figure 11(c) (ZTY coatings: 0.025, 0.056, 0.071, 0.104 mm, and 2 with 0.254 mm).

Table 5 provides a summary of the optical properties and VHT exposures for the 12 samples meeting the SDGTD requirement. Averaged values are given for the following 3 groups of samples due to similar samples displaying near identical performance: AlTi (0.025 and 0.051 mm), ZTY (0.025 to 0.104 mm) and ZTY (0.254 mm). The summary table therefore lists 7 surface treatments. Figure 12 compares the performance and VHT durability of the samples which received the 7 Haynes 188 surface treatments meeting the emittance durability requirement.

Both the 0.025 and 0.051 mm thick AlTi coatings and the 0.254 mm ZTY coating had excellent VHT performance. Because the AlTi coatings had higher initial  $\epsilon$ , slightly higher  $\epsilon$  after VHT, and received longer VHT exposure (which provided performance data earlier in the program), the AlTi coating was chosen for the  $\epsilon$  enhancement surface modification technique for the SDGTD receiver. Because both the 0.025 mm and the 0.051 mm

thick AlTi coatings performed essentially identically, the 0.025 mm coating was chosen for thermal conductivity purposes. In addition to being chosen for the receiver canisters, because of the outstanding thermal  $\epsilon$  and VHT durability, the 0.025 mm AlTi coating was also chosen for emittance enhancement for the SDGTD parasitic load radiator (PLR). The PLR functions as an electrical sink for excess power from the turboalternator/compressor, and will also be located in the thermal vacuum environment (ref. 2).

## CONCLUSIONS

Surface modification was found to increase the emittance of Haynes 188 from 0.11 to between 0.28 and 0.86. Four techniques were found to increase the  $\epsilon$  to the desired value of 0.80, or above. These techniques are: the application of an alumina-titania coating, carbon arc texturing, SiC arc texturing, and SiC grit blasting followed by air oxidation at 871 °C. The resulting  $\epsilon$  values obtained by these techniques were 0.86, 0.82, 0.80 and 0.80, respectively. Comparisons of air oxidation temperature and time, mechanical texturing versus grit blasting prior to air oxidation, AlTi and ZTY coating thicknesses, C versus SiC arc texturing, and application of a SiO<sub>2</sub> or AlO<sub>3</sub> protective coating, were individually analyzed for effects on both as-treated optical performance and VHT durability.

Of the 35 emittance enhanced Haynes 188 samples, 12 samples corresponding to 7 surface treatments were found to meet the solar dynamic ground test demonstrator VHT durability requirement ( $\epsilon \geq 0.70$  for 1 000 hr). None of the 12 samples tested were found to display any evidence of embrittlement or threat of spalling of the high emittance surface after VHT exposure with integral thermal cycling. Of the 7 surface treatments, 2 were found to display excellent VHT durability, 0.025 to 0.051 mm thick AlTi ( $\epsilon = 0.85$  after 2695 VHT hr with 32 thermal cycles) and 0.254 mm thick ZTY coatings ( $\epsilon = 0.86$  after 2024.3 hr with 25 thermal cycles). Because the AlTi coatings had higher initial  $\epsilon$ , and received longer VHT exposure (which provided performance data earlier in the program), the 0.025 mm thick AlTi coating was chosen for the  $\epsilon$  enhancement surface modification technique for the SDGTD receiver.

The success of finding a very high emittance coating which is durable to VHT will help to ensure successful demonstration of solar dynamic power generation for space applications, and has potential for applications in other systems requiring high emittance surfaces. Based on these findings, the AlTi coating has already been chosen for emittance enhancement for the SDGTD



parasitic load radiator in addition to the heat receiver canisters.

### ACKNOWLEDGMENTS

The authors would like to acknowledge several people whose help greatly contributed to this research project. We would like to thank: Dr. D. A. Gulino of Ohio University for coating samples with CVD SiO<sub>2</sub> and CVD Al<sub>2</sub>O<sub>3</sub>, Dr. R. A. Miller of NASA LeRC and G. W. Leissler of Sverdrup Technology for plasma spray coating samples with ZTY and ZYH, M. Forkapa of CSU for arc texturing samples, and C. R. Stidham for thermal analysis. Finally the authors would like to send their greatest appreciation to Dr. J. D. Whittenberger of NASA LeRC for providing the many hours of vacuum furnace exposure for our samples.

### REFERENCES

1. Labus, T.L., Secunde, R.R., and Lovely, R.G.: "Solar Dynamic Power for Space Station Freedom," Space Power, Vol. 8, Nos. 1/2, 1989, pp. 97-114.
2. Shaltens, R.K. and Boyle, R.V.: "Overview of the Solar Dynamic Ground Test Demonstration Program," Proceedings of the 28th IECEC Conference, Aug. 8-13, 1993, Atlanta, Ga., Vol. 2, pp. 2.831-2.836.
3. Strumpf, H.J. and Coombs, M.G.: "Solar Receiver for the Space Station Brayton Engine," Journal of Engineering Gas Turbines and Power, Vol. 110, April 1989, pp. 295-300.
4. Strumpf, H.J., Krystkowiak, C., and Killackey, J.J.: "Design of the Heat Receiver for the Solar Dynamic Ground Test Demonstrator Space Power System," Proceedings of the 28th IECEC Conference, Aug. 8-13, 1993, Atlanta, Ga., Vol. 1, pp. 1.469-1.474.
5. de Groh, K.K., Rutledge, S.K., Burke, C.A., Dever, T.M., Olle, R.M., and Terlep, J.A.: "Low Earth Orbit Durability Evaluation of Haynes 188 Solar Receiver Material," AIAA Paper No. 92 0850, 1992.
6. Banks, B.A., Rutledge, S.K., Mirtich, M.J., Behrend, T., Hotes, D., Kussmaul, M., Barry, J., Stidham, C., Stueber, T., and DiFilippo, F.: "Arc texturing Metals Surfaces for High Thermal Emittance Space Radiators," NASA TM-100894, 1988.
7. DiFilippo, F. and Mirtich, M.J.: "Automated Data Acquisition and Processing for a Hohlraum Reflectometer," NASA TM-101393, 1988.
8. Touloukian, Y.S., DeWitt, D.P., and Hertzberg, R.S.: Thermal Radiative Properties: Coatings, Thermophysical Properties of Matter, Vol. 9, IFI/Plenum, N.Y., 1972.
9. Kingery, W.D., Bowen, H.K., and Uhlmann, D.R.: Introduction to Ceramics, 2nd Edition, John Wiley & Sons, New York, 1976.
10. Schiroky, G.H.: "In situ measurement of silicon oxidation kinetics by monitoring spectrally emitted radiation," Journal of Materials Science, Vol. 22, 1987, pp. 3595-3601.
11. Bourgette, D.T.: "Evaporation of Iron-, Nickel-, and Cobalt-based Alloys at 760 to 980 °C in High Vacuum," ORNL-3677, 1964.



TABLE I. SUMMARY OF THE EFFECT OF SURFACE MODIFICATION ON OPTICAL PROPERTIES OF HAYNES 188

Legend	Surface treatment	Optical properties		
		$\epsilon_{827^\circ\text{C}}$	$\epsilon_{827^\circ\text{C}*}$	$\alpha_s$
Pristine	Pristine	0.14	0.08	0.370
AlTi	Alumina-titania (0.025 and 0.051 mm thick), average of 2	---	0.86	0.934
C-AT	Carbon arc textured	0.77	0.86	0.906
SiC-AT	SiC arc textured	---	0.80	0.914
871C	SiC grit blast and air oxidized (871 °C: 3, 6 and 24 hr), average of 3	0.79	0.80	0.905
ZTY	Zirconia, titania, yttria (0.025, 0.056, 0.071, 0.104 and 0.254 mm thick), average of 6	---	0.73	0.858
982C	SiC grit-blast and air oxidized (982 °C: 2, 4 and 16 hr), average of 3	0.72	0.72	0.892
Mech/Ox	Mechanically indented and air oxidized (871 °C, 24 hr)	0.68	0.67	0.890
Mech/G	Mechanically indented w/graphite application	0.42	---	0.516
ZYH	Zirconia, yttria, hafnia (0.254 mm thick), average of 2	---	0.40	0.613
Laser	Laser treated	0.28	---	0.774

TABLE II. EFFECT OF AIR OXIDATION, WITH AND WITHOUT PROTECTIVE COATINGS, ON THE OPTICAL PROPERTIES OF HAYNES 188

Surface treatment	$\epsilon_{827^\circ\text{C}}$	$\epsilon_{827^\circ\text{C}*}$	$\alpha_s$
SiC grit blast (GB) and air oxidized (871 °C, 3 hr)	0.80	0.80	0.898
SiC GB, air oxidized (871 °C/6 hr)	0.79	0.79	0.904
SiC GB, air oxidized (871 °C/24 hr)	0.77	---	0.912
Mech. indented, air oxidized (871 °C/24 hr)	0.68	0.67	0.890
SiC GB, air oxidized (982 °C/2 hr)	0.72	0.74	0.889
SiC GB, air oxidized (982 °C/4 hr)	0.72	0.70	0.893
SiC GB, air oxidized (982 °C/16 hr)	0.71	---	0.894
SiC GB, air oxidized (871 °C/3 hr), CVD SiO <sub>2</sub>	---	0.77	0.934
SiC GB, air oxidized (871 °C/6 hr), CVD SiO <sub>2</sub>	---	0.75	0.939
Mech. indent, air oxidized (871 °C/6 hr), CVD SiO <sub>2</sub>	---	0.55	0.918
SiC GB, air oxidized (871 °C/24 hr), PVD SiO <sub>2</sub>	0.80	---	0.946
SiC GB, air oxidized (871 °C/24 hr), CVD SiO <sub>2</sub> , average of 2	---	0.79	0.942
SiC GB, air oxidized (871 °C/24 hr), CVD Al <sub>2</sub> O <sub>3</sub> , average of 2	---	0.77	0.936
SiC GB, air oxidized (982 °C/2 hr), CVD SiO <sub>2</sub>	---	0.57	0.921
SiC GB, air oxidized (982 °C/4 hr), CVD SiO <sub>2</sub>	---	0.54	0.913
SiC GB, air oxidized (982 °C/16 hr), PVD SiO <sub>2</sub>	0.73	---	0.919
SiC GB, air oxidized (982 °C/16 hr), CVD SiO <sub>2</sub>	---	0.58	0.921



TABLE III. EFFECT OF ALTi OR ZTY COATING THICKNESS ON OPTICAL PROPERTIES OF HAYNES 188

Surface treatment	$\epsilon_{827^\circ\text{C}}$	$\alpha_s$
Alumina-titania (AlTi), 0.025 mm	0.86	0.935
Alumina-titania (AlTi), 0.051 mm	0.86	0.932
Zirconia, titania, yttria (ZTY), 0.025 mm	0.75	0.879
Zirconia, titania, yttria (ZTY), 0.056 mm	0.73	0.859
Zirconia, titania, yttria (ZTY), 0.071 mm	0.72	0.855
Zirconia, titania, yttria (ZTY), 0.104 mm	0.72	0.851
Zirconia, titania, yttria (ZTY), 0.254 mm average of 2	0.72	0.852

TABLE IV. EFFECT OF ARC TEXTURING, WITH AND WITHOUT PROTECTIVE COATINGS, ON THE OPTICAL PROPERTIES OF HAYNES 188

Surface treatment	$\epsilon_{827^\circ\text{C}}$	$\epsilon_{827^\circ\text{C}}$	$\alpha_s$
Carbon arc textured	0.77	0.86	0.906
SiC arc textured	---	0.80	0.914
Mechanically indented w/ graphite application	0.42	---	0.516
Carbon arc textured, PVD SiO <sub>2</sub> coated	0.80	---	0.947
Carbon arc textured, CVD SiO <sub>2</sub> coated	---	0.98	0.969

TABLE V. VACUUM HEAT TREATMENT DURABILITY PERFORMANCE OF SURFACE MODIFIED HAYNES 188

Legend	Surface treatment	VHT duration and corresponding emittance/absorptance				
AlTi	Alumina-Titania 0.025-0.051 mm thick, average of 2	0 hr $\epsilon$ : 0.86 $\alpha_s$ : 0.933	984.2 hr $\epsilon$ : 0.89 $\alpha_s$ : 0.921	1532.7 hr $\epsilon$ : 0.89 $\alpha_s$ : 0.917	2088.2 hr $\epsilon$ : 0.87 $\alpha_s$ : 0.916	2692 hr $\epsilon$ : 0.85 $\alpha_s$ : 0.915
ZTY 0.025-0.104 mm	Zirconia, titania, yttria (ZTY) 0.025-0.104 mm thick average of 4	0 hr $\epsilon$ : 0.73 $\alpha_s$ : 0.861	555.5 hr $\epsilon$ : 0.85 $\alpha_s$ : 0.923	1159.3 hr $\epsilon$ : 0.83 $\alpha_s$ : 0.922	-----	-----
ZTY 0.254 mm	Zirconia, titania, yttria (ZTY) 0.254 mm thick, average of 2	0 hr $\epsilon$ : 0.72 $\alpha_s$ : 0.852	316.5 hr $\epsilon$ : 0.89 $\alpha_s$ : 0.924	865 hr $\epsilon$ : 0.89 $\alpha_s$ : 0.926	1420.5 hr $\epsilon$ : 0.88 $\alpha_s$ : 0.936	2024.3 hr $\epsilon$ : 0.86 $\alpha_s$ : 0.938
982/16	SiC grit blast and air oxidized (982 °C, 16 hr)	0 hr $\epsilon$ : 0.71 $\alpha_s$ : 0.894	272.5 hr $\epsilon$ : 0.75 $\alpha_s$ : 0.900	940.2 hr $\epsilon$ : 0.75 $\alpha_s$ : 0.900	2044.4 hr $\epsilon$ : 0.72 $\alpha_s$ : 0.897	-----
982/16 PVD SiO <sub>2</sub>	SiC grit blast and air oxidized (982 °C, 16 hr) PVD SiO <sub>2</sub> coated	0 hr $\epsilon$ : 0.73 $\alpha_s$ : 0.921	272.5 hr $\epsilon$ : 0.78 $\alpha_s$ : 0.931	889 hr $\epsilon$ : 0.77 $\alpha_s$ : 0.920	1993 hr $\epsilon$ : 0.69 $\alpha_s$ : 0.874	-----
982/16 CVD SiO <sub>2</sub>	SiC grit blast and air oxidized (982 °C, 16 hr) CVD SiO <sub>2</sub> coated	0 hr $\epsilon$ : 0.58 $\alpha_s$ : 0.921	616.5 hr $\epsilon$ : 0.78 $\alpha_s$ : 0.938	1165 hr $\epsilon$ : 0.79 $\alpha_s$ : 0.927	1720.5 hr $\epsilon$ : 0.74 $\alpha_s$ : 0.906	2324.3 hr $\epsilon$ : 0.69 $\alpha_s$ : 0.885
982/4 CVD SiO <sub>2</sub>	SiC grit blast and air oxidized (982 °C, 4 hr) CVD SiO <sub>2</sub> coated	0 hr $\epsilon$ : 0.54 $\alpha_s$ : 0.913	616.5 hr $\epsilon$ : 0.76 $\alpha_s$ : 0.916	1165 hr $\epsilon$ : 0.69 $\alpha_s$ : 0.882	1720.5 hr $\epsilon$ : 0.56 $\alpha_s$ : 0.819	2324.3 hr $\epsilon$ : 0.43 $\alpha_s$ : 0.741



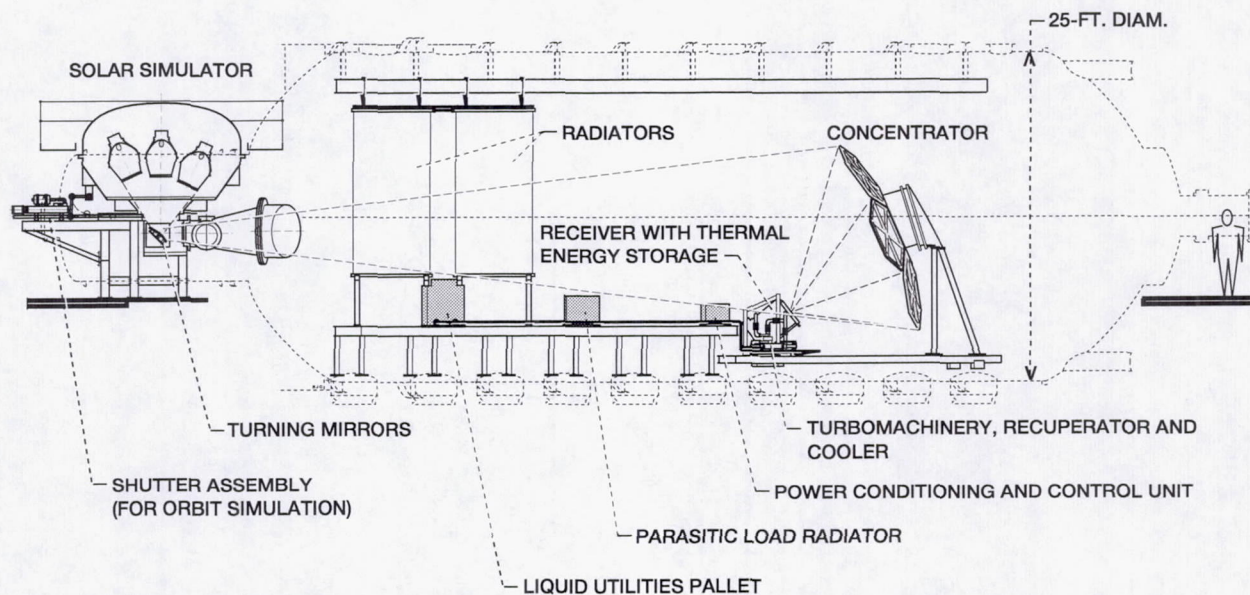


FIGURE 1. SOLAR DYNAMIC GROUND TEST DEMONSTRATOR SYSTEM IN TANK 6 AT NASA LEWIS RESEARCH CENTER.

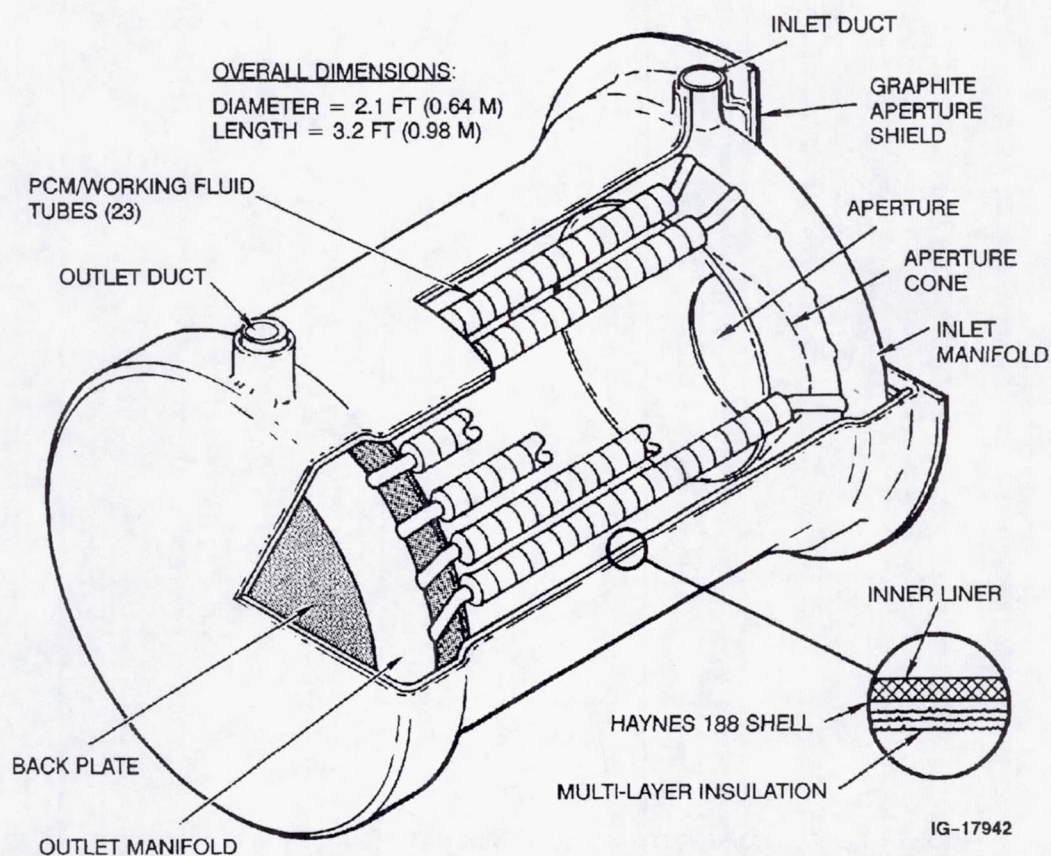


FIGURE 2. HEAT RECEIVER FOR THE 2 kW SOLAR DYNAMIC GROUND TEST DEMONSTRATOR SYSTEM.



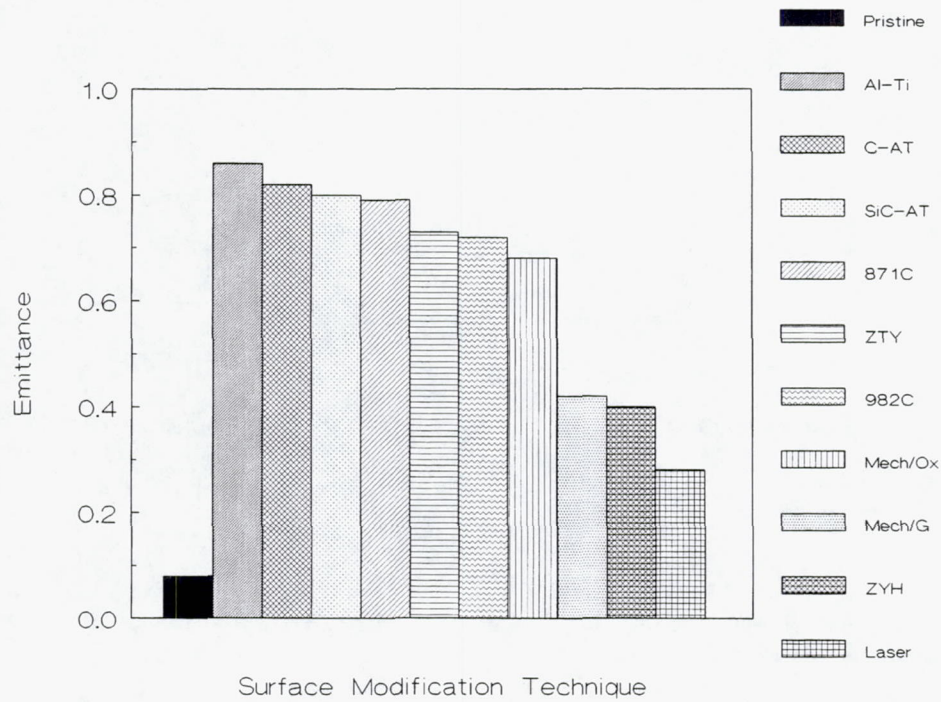


FIGURE 3. EFFECT OF SURFACE MODIFICATION ON THE EMITTANCE OF HAYNES 188.

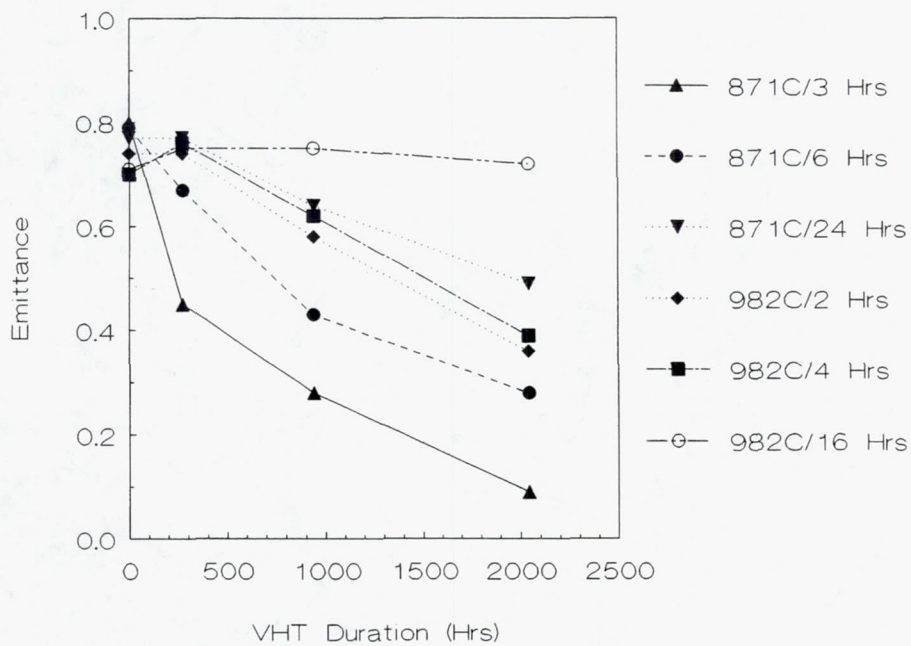


FIGURE 4. EFFECT OF AIR OXIDATION TEMPERATURE AND TIME ON THE VHT DURABILITY OF HAYNES 188.



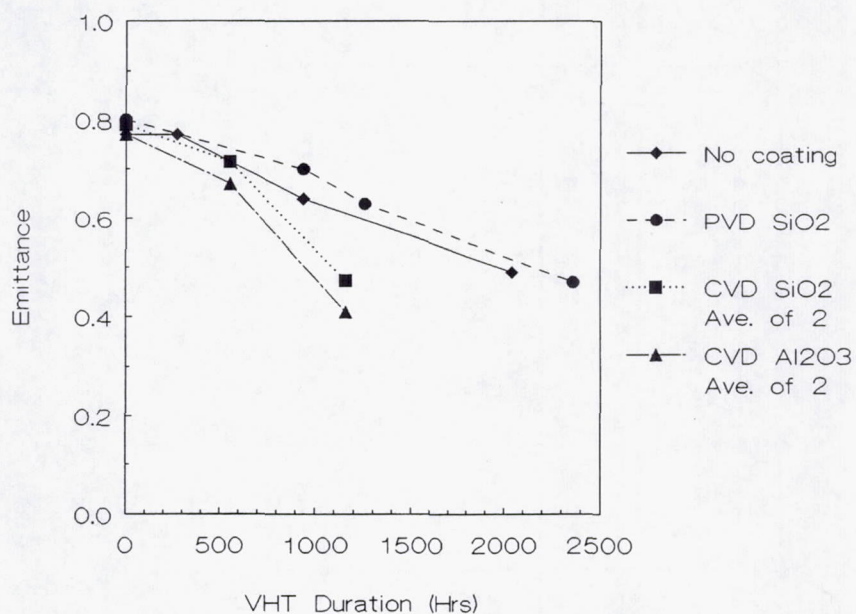


FIGURE 5. HAYNES 188 GRIT BLASTED AND AIR OXIDIZED AT 871 °C FOR 24 HOURS: COMPARISON OF THE VHT DURABILITY WITH AND WITHOUT PROTECTIVE COATINGS.

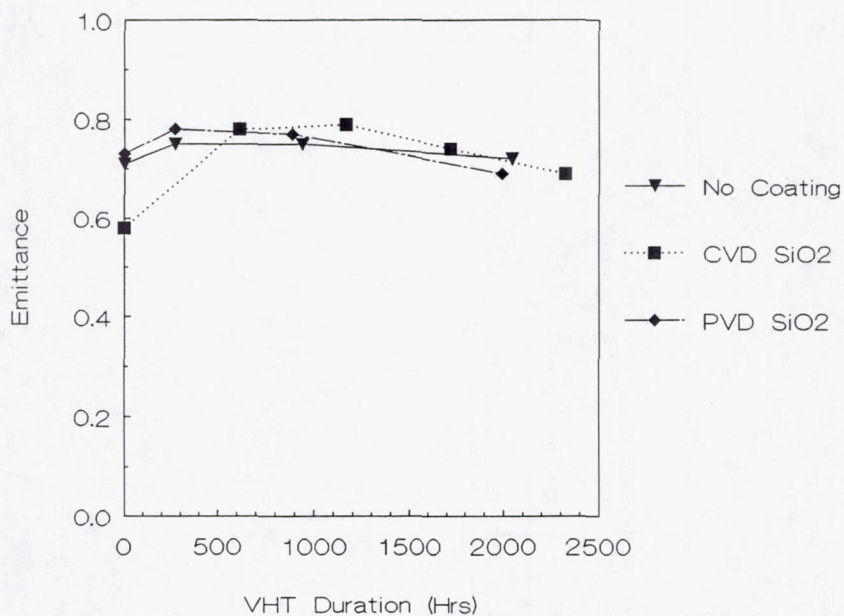


FIGURE 6. HAYNES 188 GRIT BLASTED AND AIR OXIDIZED AT 982 °C FOR 16 HOURS: COMPARISON OF THE VHT DURABILITY WITH AND WITHOUT PROTECTIVE COATINGS.



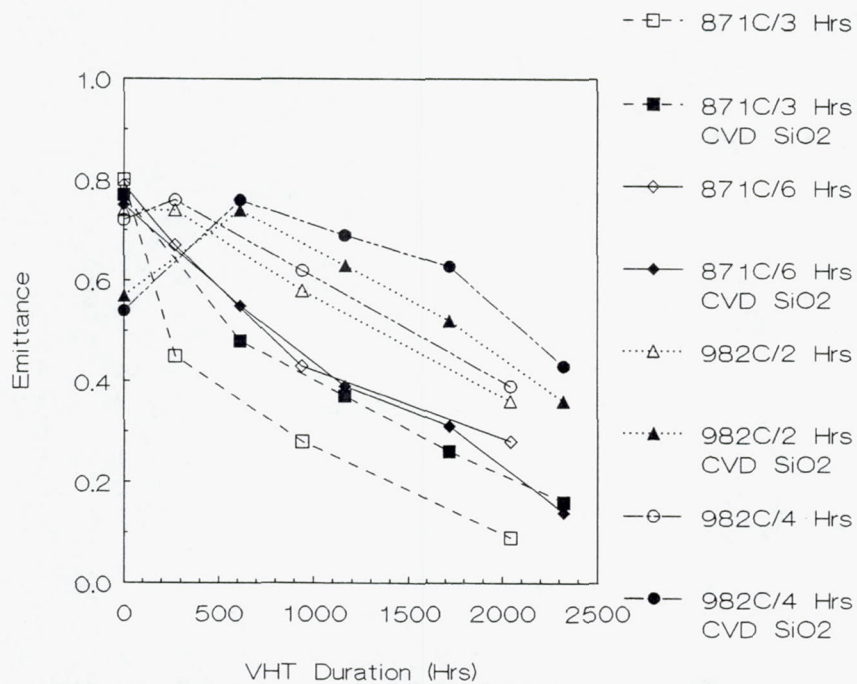


FIGURE 7. HAYNES 188 GRIT BLASTED AND AIR OXIDIZED FOR SHORT DURATIONS: COMPARISON OF THE VHT DURABILITY WITH AND WITHOUT PROTECTIVE COATINGS.

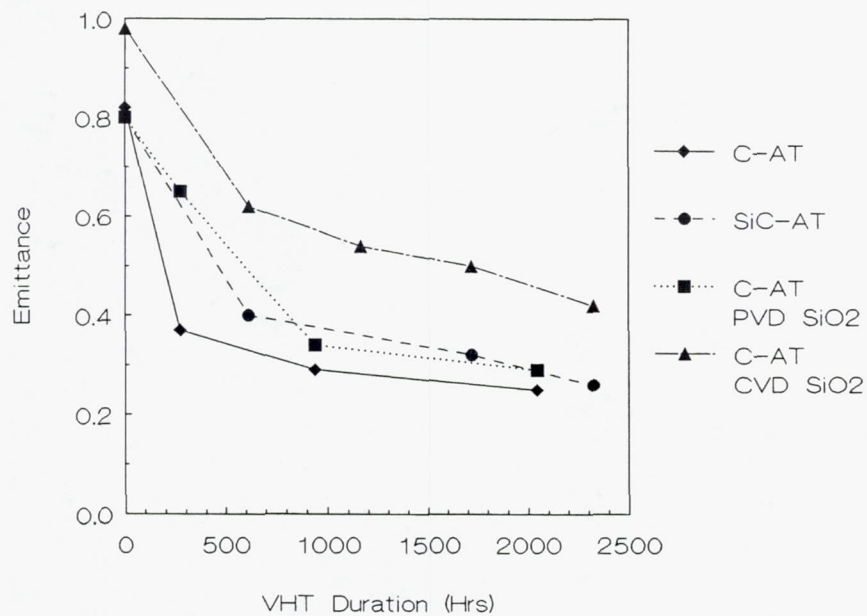


FIGURE 8. COMPARISON OF C AND SiC ARC TEXTURING AND THE EFFECTIVENESS OF PROTECTIVE COATINGS ON C ARC TEXTURED HAYNES 188.



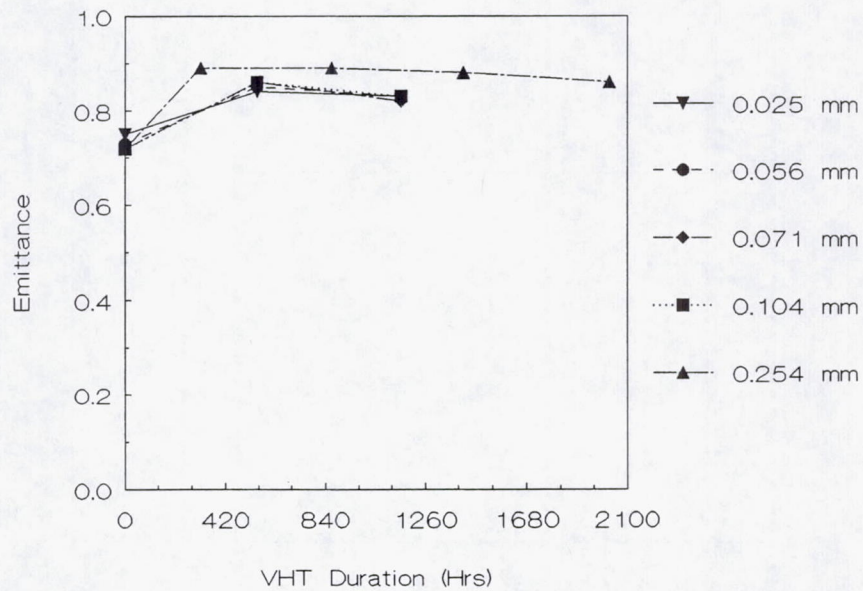


FIGURE 9. EFFECT OF COATING THICKNESS ON THE VHT DURABILITY OF ZTY COATED HAYNES 188.

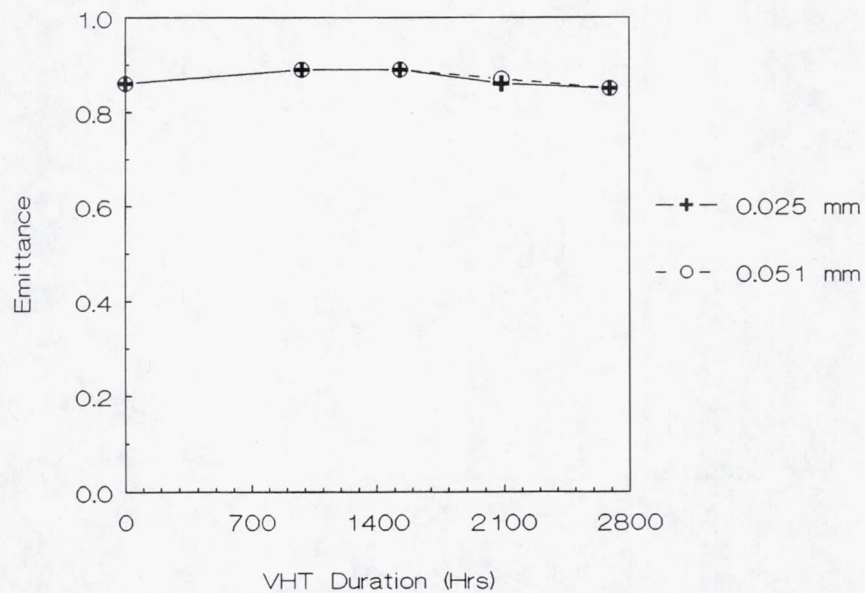


FIGURE 10. EFFECT OF COATING THICKNESS ON THE VHT DURABILITY OF AlTi COATED HAYNES 188.



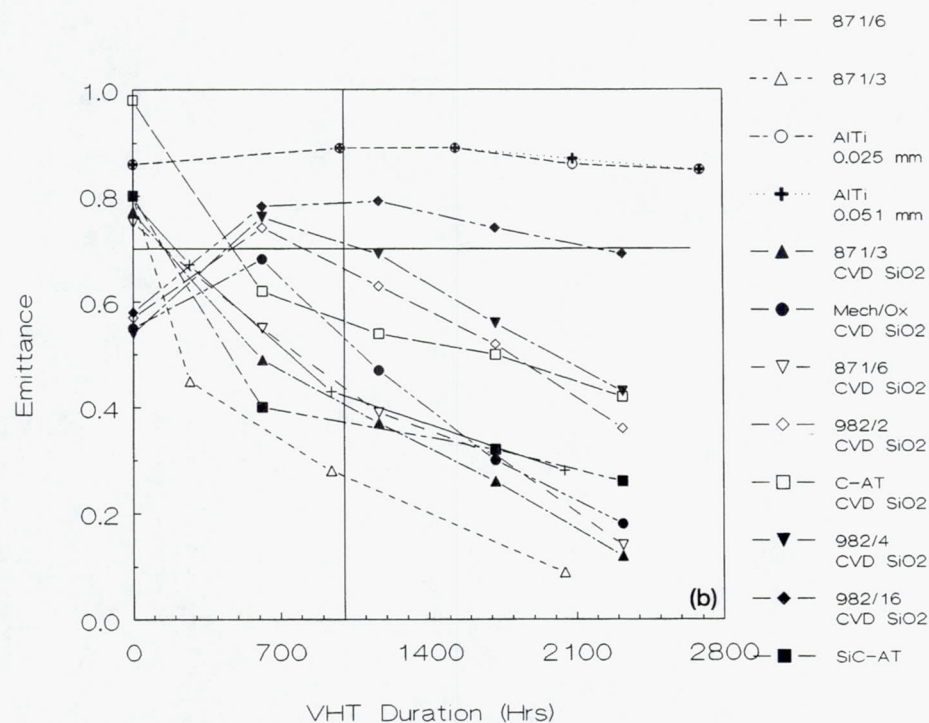
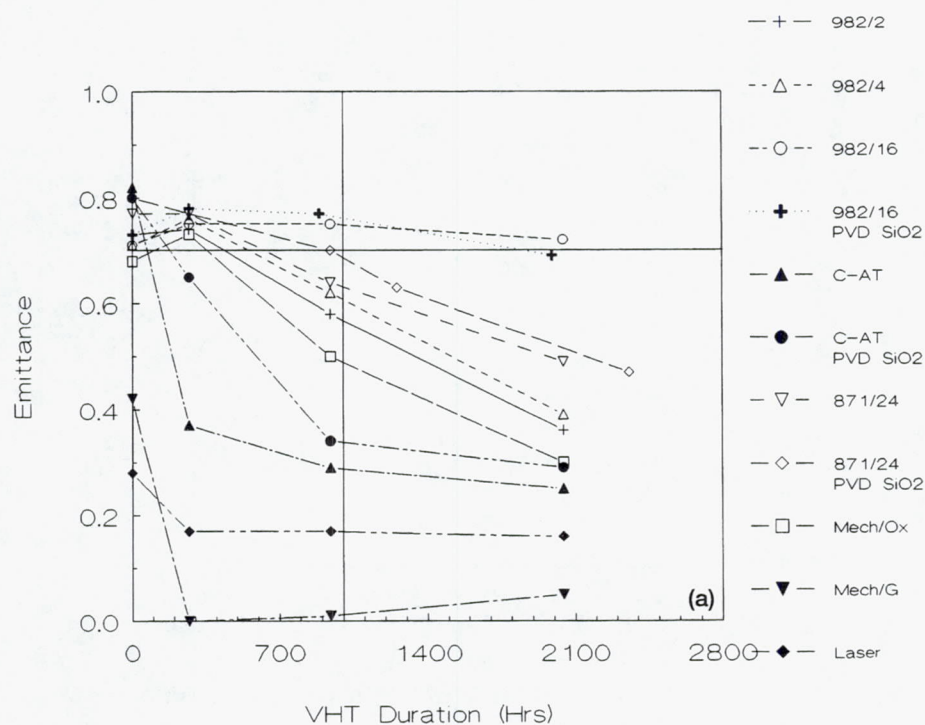


FIGURE 11. PERFORMANCE COMPARISON OF THE VHT DURABILITY OF VARIOUS SURFACE TREATED HAYNES 188 SAMPLES. SDGTD REQUIRES AN EMITTANCE OF AT LEAST 0.7 AFTER 1000 HOURS VHT EXPOSURE.



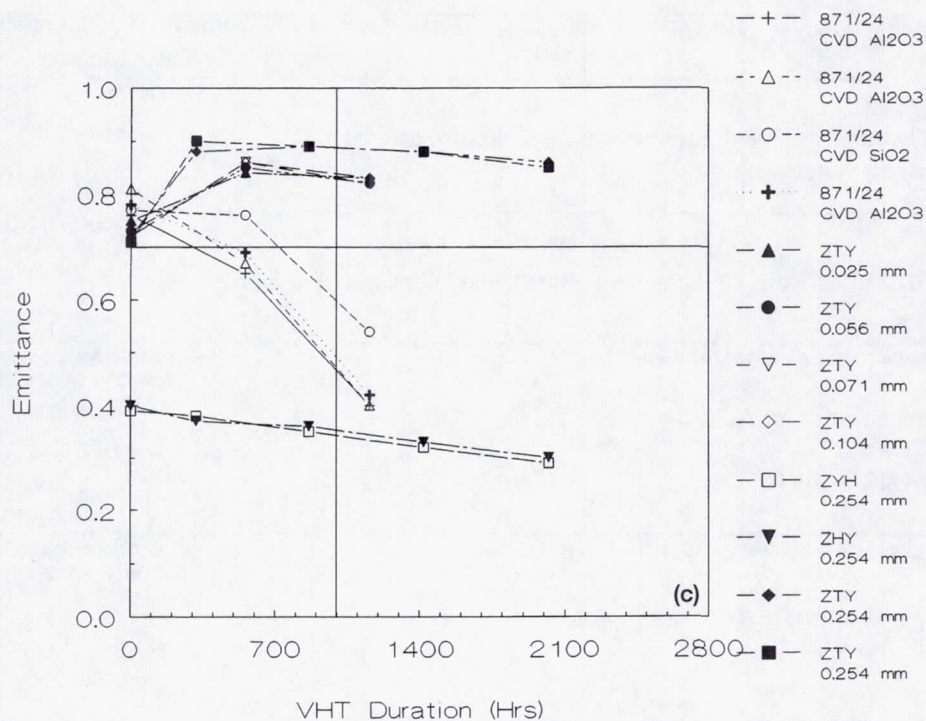


FIGURE 11. CONCLUDED.

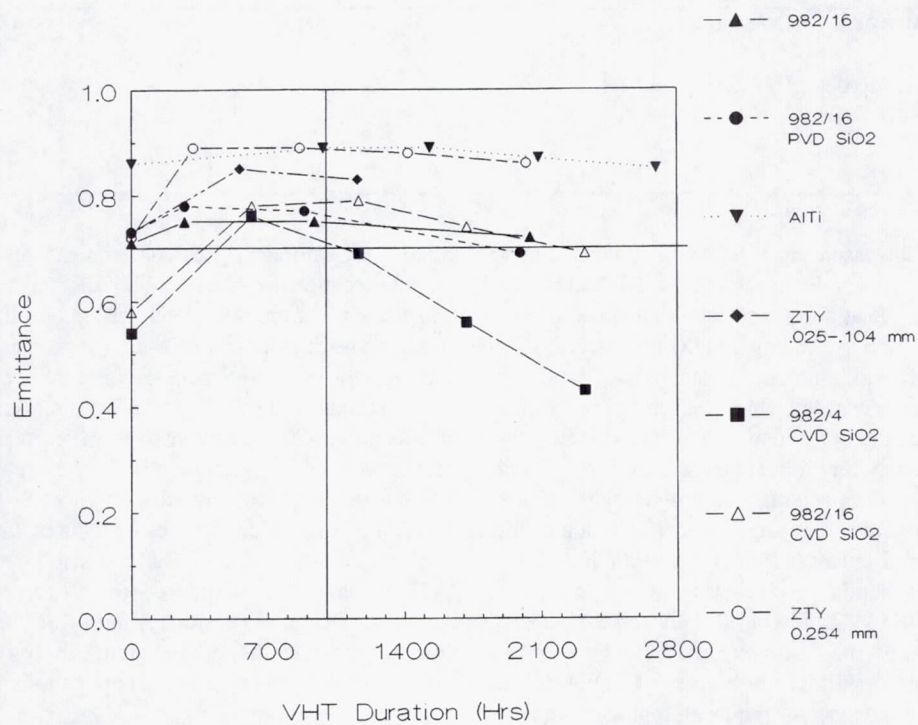


FIGURE 12. PERFORMANCE COMPARISON OF THE 7 SURFACE TREATMENTS WHICH MET THE SDGTD EMITTANCE PERFORMANCE REQUIREMENT AFTER 1000 HOURS OF VHT EXPOSURE.



REPORT DOCUMENTATION PAGE			Form Approved OMB No. 0704-0188	
Public reporting burden for this collection of information is estimated to average 1 hour per response, including the time for reviewing instructions, searching existing data sources, gathering and maintaining the data needed, and completing and reviewing the collection of information. Send comments regarding this burden estimate or any other aspect of this collection of information, including suggestions for reducing this burden, to Washington Headquarters Services, Directorate for Information Operations and Reports, 1215 Jefferson Davis Highway, Suite 1204, Arlington, VA 22202-4302, and to the Office of Management and Budget, Paperwork Reduction Project (0704-0188), Washington, DC 20503.				
1. AGENCY USE ONLY (Leave blank)	2. REPORT DATE March 1997	3. REPORT TYPE AND DATES COVERED Technical Memorandum		
4. TITLE AND SUBTITLE  Performance and Durability of High Emittance Heat Receiver Surfaces for Solar Dynamic Power Systems		5. FUNDING NUMBERS  WU-585-03-21		
6. AUTHOR(S)  Kim K. de Groh, David M. Roig, Christopher A. Burke, and Dilipkumar R. Shah				
7. PERFORMING ORGANIZATION NAME(S) AND ADDRESS(ES)  National Aeronautics and Space Administration Lewis Research Center Cleveland, Ohio 44135-3191		8. PERFORMING ORGANIZATION REPORT NUMBER  E-8700		
9. SPONSORING/MONITORING AGENCY NAME(S) AND ADDRESS(ES)  National Aeronautics and Space Administration Washington, D.C. 20546-0001		10. SPONSORING/MONITORING AGENCY REPORT NUMBER  NASA TM-106549 Revised Copy		
11. SUPPLEMENTARY NOTES Prepared for the 1994 ASME International Solar Energy Conference sponsored by the American Society of Mechanical Engineers, San Francisco, California, March 27-30, 1994. Kim K. de Groh, NASA Lewis Research Center; David M. Roig and Christopher A. Burke, Cleveland State University, Cleveland, Ohio 44115; and Dilipkumar R. Shah, AlliedSignal Aerospace Company, Torrance, California 90509. Responsible person, Kim K. de Groh, organization code 5480, (216) 433-2297.				
12a. DISTRIBUTION/AVAILABILITY STATEMENT  Unclassified - Unlimited Subject Category 20		12b. DISTRIBUTION CODE		
13. ABSTRACT (Maximum 200 words)  Haynes 188, a cobalt-based superalloy, will be used to make thermal energy storage (TES) containment canisters for a 2 kW solar dynamic ground test demonstrator (SDGTD). Haynes 188 containment canisters with a high thermal emittance ( $\epsilon$ ) are desired for radiating heat away from local hot spots, improving the heating distribution, which will in turn improve canister service life. In addition to needing a high emittance, the surface needs to be durable in an elevated temperature, high vacuum ( $\approx 830^\circ\text{C}$ , $<10^{-7}$ torr) environment for an extended time period. Thirty-five Haynes 188 samples were exposed to 14 different types of surface modification techniques for emittance and vacuum heat treatment (VHT) durability enhancement. Optical properties were obtained for the modified surfaces. Emittance enhanced samples were exposed to VHT for up to 2692 hours at $827^\circ\text{C}$ and $\leq 10^{-6}$ torr with integral thermal cycling. Optical properties were taken intermittently during exposure, and after final VHT exposure. The various surface modification treatments increased the emittance of pristine Haynes 188 from 0.11 to between 0.86. Seven different surface modification techniques were found to provide surfaces which met the SDGTD receiver VHT durability requirement ( $\epsilon \geq 0.70$ after 1000 hrs). Of the 7 surface treatments, 2 were found to display excellent VHT durability: alumina-titania (AlTi) coatings ( $\epsilon = 0.85$ after 2695 VHT hrs) and zirconia-titania-yttria coatings ( $\epsilon = 0.86$ after 2024.3 VHT hrs). The AlTi coating was chosen for the $\epsilon$ enhancement surface modification technique for the SDGTD receiver. Details of the alumina-titania coating and other Haynes 188 emittance surface modification techniques are discussed. Technology from this program will lead to successful demonstration of solar dynamic power for space applications, and has potential for application in other systems requiring high emittance surfaces.				
14. SUBJECT TERMS  Thermal emittance; Solar absorptance; Vacuum heat treatment; Haynes 188; Solar dynamic ground test demonstrator; Surface modification			15. NUMBER OF PAGES 20	
			16. PRICE CODE A03	
17. SECURITY CLASSIFICATION OF REPORT Unclassified	18. SECURITY CLASSIFICATION OF THIS PAGE Unclassified	19. SECURITY CLASSIFICATION OF ABSTRACT Unclassified	20. LIMITATION OF ABSTRACT	